ELSEVIER

Thermochimica Acta 246 (1994) 81–97

thermochimica acta

Thermal analysis of new glass ceramic composite tapes and their components

D. Schultze *, W. Schiller, E. Schiller

Bundesanstalt für Materialforschung und -prüfung, Zweigstelle Berlin-Adlershof, Labor 10.34, Rudower Chaussee 5, D-12489 Berlin, Germany

Received 10 January 1994; accepted 11 March 1994

Abstract

Glass ceramic tapes prepared from various AlN, glass and organic binders were studied by simultaneous TG–DTA. Thermooxidative decomposition of polymeric binder, dehydration, oxidation of residual carbon, glass crystallization and oxidation of AlN were detected and evaluated. Results are compared with those obtained with the pure components AlN and glass.

The rate of oxidation of various AlN charges at $> 800°C$ in an air flow depends on their specific surface and eventual special (antihydrolytic) coating. In the ceramic composite the oxidation of AlN is much slower than in free AlN powder because of the embedding in the glass matrix.

The glass exhibits crystallization to cordierite, the crystallization rate and final crystallinity depending on the P_2O_5 and B_2O_3 contents and the particle size of the glass. In the composite the crystallization of the glass component is accelerated and proceeds to a higher degree owing to the smaller particle size and to interactions between glass and filler. Grinding of the ceramic raw mix results in additional adsorption of moisture.

Keywords: Aluminium nitride; Ceramic; Coupled technique; Crystallization; Glass; Tape

1. Introduction

Glass ceramic composite tapes consisting of silicate glass, inorganic filler (e.g. Al_2O_3) and an organic binder system of polymer and plasticizer are used as

* Corresponding author.

SSDI 0040-6031(94)01791-E

multilayer substrates for electronic circuits [1–3]. To improve the performance of such circuits, the dissipation of (Joule) heat losses, i.e. heat conduction from the interior to the surface, has to be improved. This is possible by (a) increasing the (intrinsic) thermal conductivity of the composite and/or its components, and/or (b) minimizing the porosity in the fired ceramic composite.

Object (a) is achieved, for example, by substituting AlN (specific thermal conductivity $\lambda_{AlN} \approx 200$ W K^{-1} m^{-1}) for Al_2O_3 ($\lambda_{Al_2O_3} \approx 20$ W K^{-1} m^{-1}) or SiO_2 ($\lambda_{SiO_2} \approx 10$ W K^{-1} m^{-1}); (b) is improved by appropriately selecting the binder material and glass and establishing a firing procedure that avoids gas evolution during or after sintering of the composite.

Thermal analysis has been applied to study both the behaviour of the components AlN and glass alone and their interaction in the firing process of the composite tapes. This process must be carried out in such way that the organic binder is totally oxidized to leave no carbonaceous residue which could reduce the molten oxide glass with formation of CO/CO_2 gas bubbles. On the other hand, oxidation of AlN by atmospheric oxygen has to be avoided. The results to be presented here allow conclusions to be drawn concerning the technology of glass ceramic composite tapes.

2. Experimental

2.1. Materials

Aluminium nitride

Six AlN charges (Table 1) of different particle sizes obtained from three commercial manufacturers were tested. Unlike the other products, charge WF was surface coated by the manufacturer to prevent hydrolysis.

Table 1
AlN samples

Sample	Particle size distribution [a]			F_{BET}/ (m^2 g^{-1})	Manufacturer	(brand)
	d_{90}/ (μm)	d_{50}/ (μm)	d_{10}/ (μm)			
F/S	2.8	1.8	0.8	3.4	Tokuyama Soda	(grade F)
B	5.6	1.9	0.7	3.4	H.C. Starck	(grade B)
WF	7.2	2.8	0.5	3.4 [b]	Toyo Aluminium	(Toyalnite WF)
UF	7.2	2.8	0.5	3.5	Toyo Aluminium	(Toyalnite UF)
A	14	5.4	2.5	1.2	H.C. Starck	(grade A)
UM	20	7.3	2.6	0.9	Toyo Aluminium	(Toyalnite UM)

[a] Determined by Sedigraph 5000, Micromeritics Co.
[b] Surface coated to prevent hydrolysis.

Table 2
Composition of glasses. Compositions are given in mol% as determined by chemical analysis of the glass after melting

Sample	Cordierite base glass $MgO/Al_2O_3/SiO_2$	P_2O_5	B_2O_3
B 5/1	91.7	0.83	8.0
B 7/2.3	93.7	0.90	5.2
B 7/1	93.7	0.77	5.0
B 9/1	92.7	2.0	5.0
B 10	94.2	0.81	5.0
B 2/1	94.4	0.64	4.8
B 3/1	95.2	0.06	4.7
B 8/1	95.5	0.8	3.6

Glasses

Cordierite-forming glasses (Table 2) containing different admixtures of B_2O_3 and P_2O_5 were synthesized by conventional melting at 1500–1600°C and quenching or drawing. They were ground and different size fractions were sieved.

Polymer binders

Binders contained either poly(vinylbutyral) (PVB) or a polyacrylate (PAcr) mixture as polymeric base component and butyl phthalate as plasticizer, dissoved in ethanol/ketone mixtures as solvent.

Tapes

Mixtures of AlN ($\approx$ 30 vol%) and glass ($\approx$ 70 vol%) were ground by ball milling in the solvent with addition of a dispersant. This raw mix was suspended in the binder and $\approx$ 200 μm thick tapes were formed by the doctor blade technique and subsequent drying. Table 3 presents the composition of a typical tape.

2.2. Procedure

The measurements were performed in a SETARAM TAG 24 thermoanalyzer with simultaneous TG/DTA recording. The sample was placed in a 100 μl platinum crucible, using an empty crucible as reference. The atmosphere was flowing air, eventually N_2, at > 500°C. Since even small amounts of oxygen in the atmosphere can drastically affect the thermal behaviour of ceramic/binder systems [4], the thermobalance was evacuated to 0.1 mbar before filling and flushing with 99.99% N_2 gas.

Table 3
Starting mixture to prepare a glass ceramic composite type

Ceramic powder	30 vol% AlN, 70 vol% glass	68–72 vol%
Binder	poly(vinylbutyral) or polyacrylate plus plasticizer	28–32 vol%
Dispersant	amount depending on particle size	0.2–0.6 vol%

The green tape was cut into fragments of area ≈ 6 mm^2 and 200 μm thick. Sample masses were: tape or AlN, ≈ 50 mg; glass, ≈ 22 mg. The heating rate was 5 K min^{-1} to 1150°C; with the tapes, heating was stopped at ≈ 500°C to allow combustion of the carbonaceous residues of organic components, and then continued to 1150°C. Subsequently, the dead-burnt sample was subjected to a second heating cycle. For evaluation, results from the second cycle were subtracted from those of the first to cancel out apparatus factors (buoyancy, and temperature-dependent drift of the DTA curve).

3. Results and discussion

3.1. Aluminium nitride

The aluminium nitride charges under investigation may be roughly divided into two groups with specific surfaces of either ≈ 1 or ≈ 3.4 m^2 g^{-1}. The various AlN samples exhibit small mass losses between room temperature and a shallow mass minimum at 500 to 800°C, followed by strong exothermal mass gain at > 750°C (Figs. 1 and 2 and Table 4).

Behaviour below 750°C

Mass losses up to the minimum amounted to 0.07–0.34%. In general, the AlN charges with the larger specific surface exhibited the greater mass losses. This indicates that this mass loss is a surface phenomenon, probably desorption and

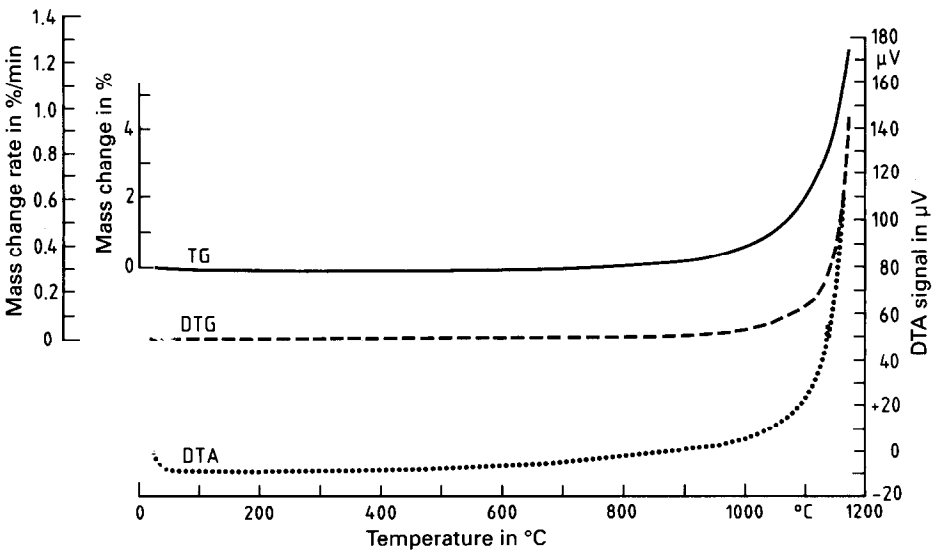

Fig. 1. TG, DTG and DTA curves of an AlN sample in air.

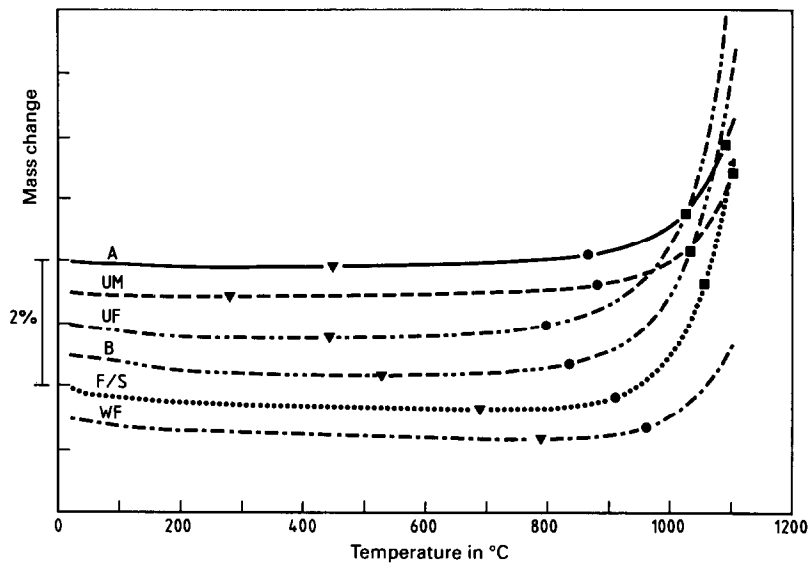

Fig. 2. TG curves (in air) of the AlN samples of Table 1. The symbols on each curve represent, respectively, ▼, Point of mass minimum, ●, $T_{0.2\%}$, point of 0.2% mass increase after mass minimum, ■, $T_{2\%}$, point of 2% mass increase after mass minimum.

Table 4
Characteristic results of thermal analysis of AlN charges

Sample	F/S	B	WF	UF	A	UM
Specific surface $F_{BET}/(m^2\ cm^{-3})$	3.4	3.4	3.4	3.5	1.2	0.9
Mass loss to minimum/(%)	0.34	0.33	0.34	0.21	0.10	0.07
Temperature of mass gain:						
0.2% from minimum $T_{0.2\%}/(°C)$	916	836	964	793	856	882
2% from minimum $T_{2\%}/(°C)$	1056	1033	1122	1025	1087	1102
Mass gain from 950–1050°C $\delta m_{1000°C}/(\%)$	1.46	1.82	0.62	1.88	0.82	0.67

evolution of water, eventually coupled with some hydrolysis of AlN and subsequent dehydration of aluminium hydroxides. In contrast to the other AlN charges, AlN WF shows mass losses continuing to a mass minimum at 700–800°C. Possibly the thermal degradation of the surface coating material extends over a wide temperature interval. A similar, less pronounced tendency was shown by AlN charge F/S.

Mass gain above 750°C

Above 750°C AlN is oxidized to Al_2O_3. The onset of AlN oxidation after the mass minimum is very gradual. Therefore, instead of an onset temperature, the temperatures corresponding to 0.2 and 2% mass increase above the mass minimum ($T_{0.2\%}$, $T_{2\%}$) were selected as characteristic parameters to describe the beginning of

the oxidation, together with the mass increase (in percent) between 950 and 1050°C ($\delta m_{1000°C}$) as a measure of the oxidation rate at comparable temperature. The oxidation of AlN is not complete at 1150°C but occurs at an ever-increasing rate.

The oxidation of those aluminium nitrides with larger specific surfaces starts at a lower temperature and proceeds at a higher rate, as indicated by the data of $T_{0.2\%}$, $T_{2\%}$ and $\delta m_{1000°C}$. Again, AlN charge WF is an exception: even though it belongs to the group with larger specific surface, its oxidation starts at the highest temperature and the reaction rate $\delta m_{1000°C}$ is the lowest for all the samples. Obviously the antihydrolytic surface coating also restricts the high-temperature oxidation. Probably this coating consists of a hydrophobic organosilicon compound and is thermooxidatively decomposed at $> 300°C$ to form a thin SiO_2 film that protects the AlN against oxidation.

Compared with AlN charges UF and B of comparable specific surface, the AlN charge F/S shows restricted oxidation. This, together with the behaviour at $< 750°C$ suggests that the latter charge has surface protection similar to, but less effective than, that of AlN charge WF.

3.2. Glasses

Glasses of the system $MgO/Al_2O_3/SiO_2$ with various admixtures are well known to exhibit crystallization of cordierite $Mg_2Al_3(AlSi_5)O_{18}$ [5]. With some specific agents in the glass, e.g. TiO_2, ZrO_2, Li_2O, F^- or P_2O_5, and after proper preheating, this crystallization proceeds heterogeneously with volume nucleation [6,7]. Without such agents present, or with admixtures of B_2O_3 or P_2O_5, the crystallization is nucleated from the glass particle surface [8,9]. The role of P_2O_5 is interpreted in various ways; probably it depends on the composition of the parent glass as well as on the P_2O_5 content. Thus we have to anticipate that the particle size and the B_2O_3 and P_2O_5 contents of the glass affect the crystallization process. From various glass compositions and powder fractions we have estimated the influence of these factors.

The crystallization of the cordierite phase is manifested by an exothermal DTA effect, without any accompanying mass change, around 920–1040°C, in good agreement with [8]. For comparison we have evaluated the extrapolated onset temperature T_e and the peak temperature T_p, peak heights and peak areas δH of the DTA effects.

With increasing contents of B_2O_3 (Fig. 3, Table 5) the crystallization peak is shifted to higher temperatures, the thermal effect is flattened and the crystallization heat (peak area) becomes smaller.

An increase in the P_2O_5 content affects the crystallization in an ambiguous manner (Fig. 4, Table 6). The peak temperature is increased at low P_2O_5 concentrations and decreased at higher P_2O_5 concentrations; the exothermic crystallization peak areas become larger at low P_2O_5 concentrations and smaller at higher P_2O_5 concentrations. These results are further modified by the influence of the particle size of the glass.

At smaller particle size (Fig. 5, Table 6) the crystallization is shifted to lower temperatures and the peak area and peak height of the DTA effect are

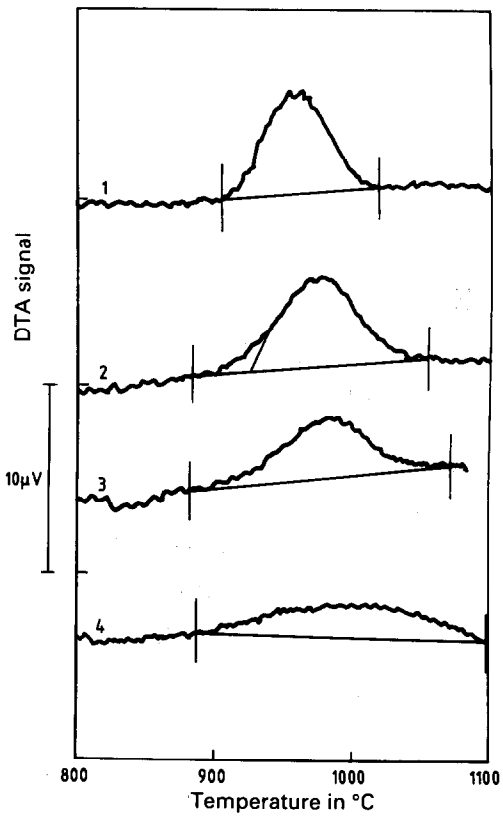

Fig. 3. DTA curves of cordierite crystallization of glasses (Table 5) of different B_2O_3 contents. 1, glass B 8/1; 2, glass B 2Pt1; 3, glass B 7/1; 4, glass B 5/1.

Table 5
Effect of B_2O_3 content on the crystallization of glasses

Type	Glass		Crystallization exotherm	
	Contents		Peak maximum temperature T_p/(°C)	Peak area δH/(mV s g^{-1})
	B_2O_3/ (mol%)	P_2O_5/ (mol%)		
B 8/1	3.6	0.8	961	170
B 2Pt1	4.8	0.64	978	157
B 7/1	5.0	0.77	988	125
B 5/1	8.0	0.83	1013	114

increased. This effect of the particle size is somewhat different for the various glass compositions, and the shift of T_p is more distinct for the glasses with lower P_2O_5 contents.

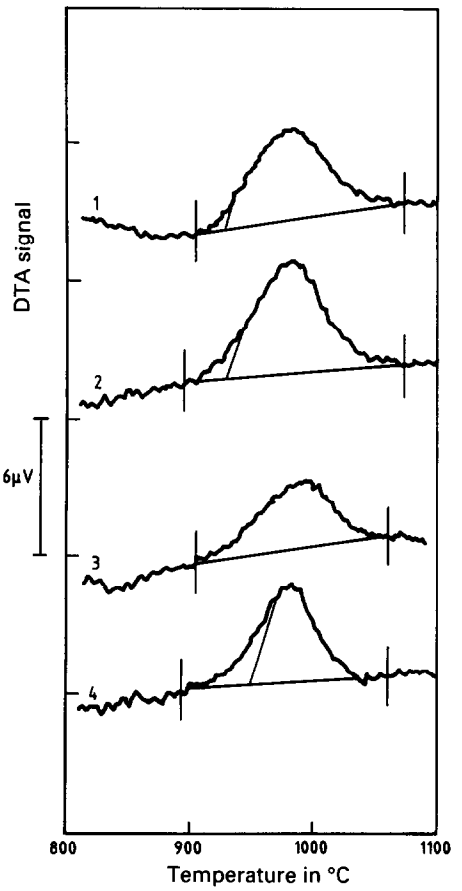

Fig. 4. DTA curves of cordierite crystallization of glasses of different P_2O_5 contents (Table 6). 1, glass B 3/1; 2, glass B 2Pt1; 3, glass B 7/1; 4, glass B 9/1.

3.3. Tape composites

Firing of green tapes to the glass ceramic composite involves several processes, some of them clearly distinguished by their thermal effects (Fig. 6):

(a) evaporation of residual binder solvent;
(b) decomposition and oxidation (burnout) of organic binder;
(c) oxidation of residual carbon;
(d) glass transition of the glass component
(e) oxidation of AlN;
(f) crystallization of cordierite from the glass matrix.

Small mass losses of $< 1\%$ below 150°C can be ascribed to the evaporation of residual solvent. However, the mass loss rate gradually increases up to the beginning of binder burnout, so there is no distinct separation between these processes.

Table 6
Effect of P_2O_5 content and particle size on the crystallization of glasses

Type	Glass			Crystallization exotherm	
	Contents		Particle size/ (μm)	Peak maximum temperature T_p/(°C)	Peak area δH/(mV s g^{-1})
	P_2O_5/ (mol%)	B_2O_3/ (mol%)			
B 3/1	0.06	4.7	>40	972	140
			<40	928	150
B 2Pt1	0.64	4.8	>40	978	157
			<40	960	155
B 7/1	0.77	5.0	>40	988	125
			<40	972	131
B 9/1	2.0	5.0	>40	979	132
B 9/2U	2.0	5.0	>40	945	115
			<40	950	128

3.4. *Burnout of binder*

The thermooxidative decomposition of organic binders in air gives rise to exothermal effects and mass losses. The two binders under study exhibit characteristically different TG–DTA patterns (Fig. 7).

Poly(vinyl butyral) (PVB) binder

Burning proceeds in three overlapping exothermic steps peaking at ≈220, ≈280 and ≈480°C, respectively. Frequently an endothermic peak is found at ≈265°C, where the mass loss rate exhibits a maximum. The shape and area of the individual DTA partial peaks and the associated mass losses are poorly reproducible. Generally the mass loss rate becomes lower at the transition from the endotherm to the second exotherm and during the latter. The third exothermic effect is clearly associated with a second, smaller TG step. Around 500°C, exothermic processes and mass losses are essentially concluded (however, see section 3.5).

Polyacrylate (PAcr) binder

Combustion consists of a two-step mass loss; the first step (≈150–270°C, mass loss ≈7%) shows a weak, broad endothermic effect, whereas the second step (≈11%) always shows an intense exotherm, frequently preceded by an endothermic minimum at the temperature of the maximum mass loss rate. Mass loss steps are clearly reproducible, but the reproducibility of the DTA curve is poorer. Both mass loss and exothermic effect end around 450°C, about 50 K lower than the oxidative degradation of the PVB binder.

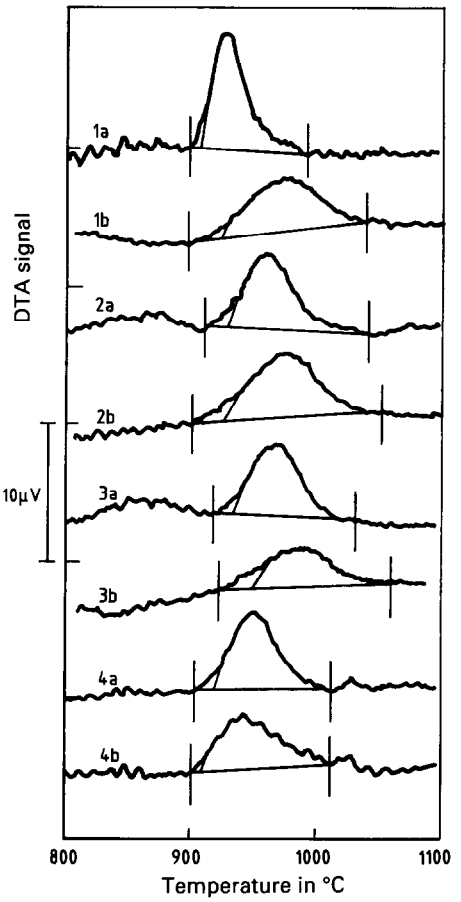

Fig. 5. DTA curves of cordierite crystallization of glasses of different particle sizes (Table 6). 1a, 2a, 3a, 4a, particle size < 40 µm; 1b, 2b, 3b, 4b, particle size > 40 µm; 1a, 1b, glass B 3/1; 2a, 2b, glass B 2Pt1; 3a, 3b, glass B 7/1, 4a, 4b, glass B 9/2U.

To explain the poor reproducibility of DTA curves of the thermooxidative degradation of the binders, one has to consider the complex nature of these processes. In the thermooxidative degradation of polymers there occur different types of chemical reactions, simultaneously or consecutively, resulting in characteristic thermoanalytical features:

(a) oxidation of polymer; addition of oxygen without destruction of the polymer backbone: exothermal, small mass gain;

(b) thermal depolymerization of unchanged or oxidized polymer and volatilization of low-molecular weight fragments: strong endothermal, mass loss;

(c) oxidation of volatile fragments with air: strongly exothermal, mass loss due to preceding step (b).

There are no data suggesting that (a) plays any role in the combustion of our binders. Instead, the burnout behaviour is determined by reaction types (b) and (c),

Table 7
Thermal analysis results of ceramic tapes prepared from different AlN charges with the same glass, B 7/2.3

AlN charge	F/S	B	WF	UF	A	UM	Glass [a]
$F_{BET}/(m^2\ cm^{-3})$	11.6	11.0	10.8	10.5	7.3	6.8	9.4
mass losses/(%)							
<150°C	0.27	0.37	0.32	0.32	0.24	0.26	
150–440°C	22.11	20.37	20.11	19.82	18.22	18.50	
440–507°C	0.25	0.12	0.10	0.08	0.08	0.08	
507–750°C	0.11	0.03	0.04	0.03	0.03	0.04	
mass gain/(%)							
750–1150°C	0.10	0.05	0.06	0.05	0.08	0.05	
glass crystallization							
$T_e/(°C)$	939	940	943	941	950	951	950
$T_p/(°C)$	965	966	970	967	980	980	981
DTA peak area $\delta H/$							
(mV s g^{-1} tape)	86	80	83	73	55	58	129
(mV s g^{-1} glass)	172	155	163	142	108	110	129

[a] Glass B 7/2.3V15 was used to prepare the tapes in this list. For comparison with the tapes it was ground to a similar particle size.

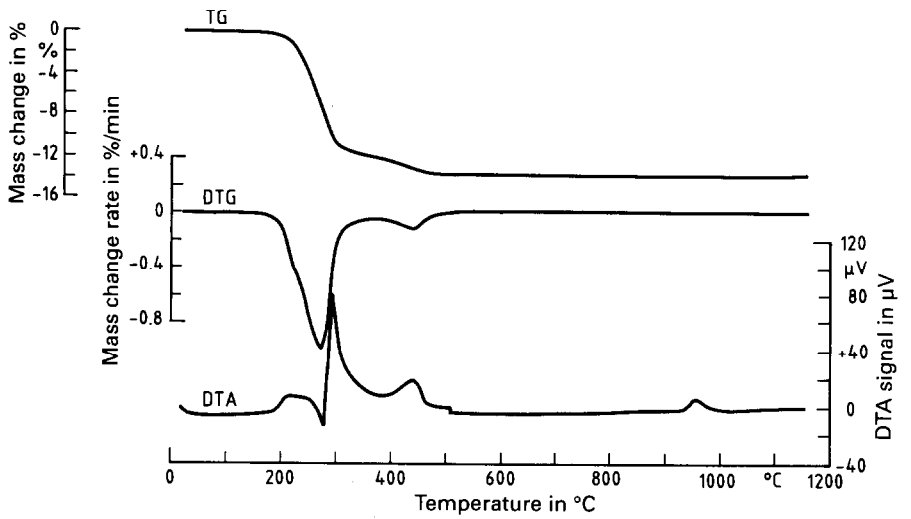

Fig. 6. TG, DTG and DTA curves (in air) of a green ceramic composite tape containing poly(vinylbutyral) binder. Programmed heating was interrupted by an isothermal hold at 507°C for 1 h.

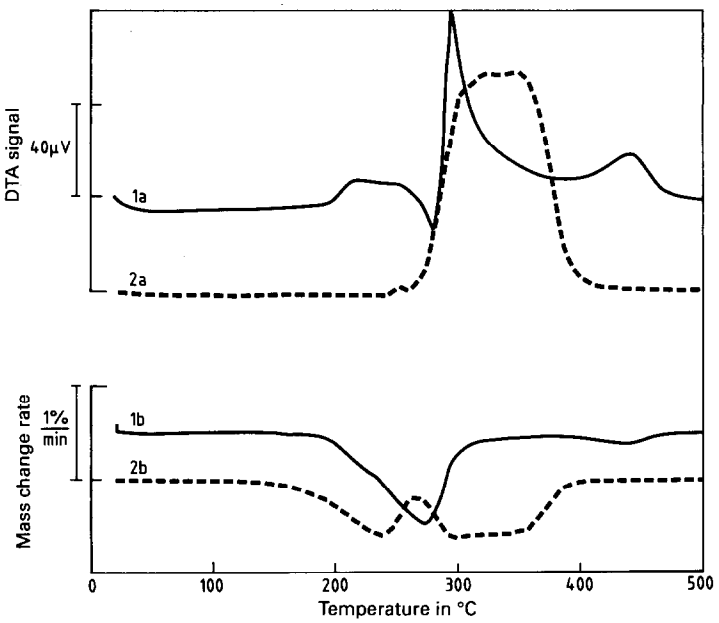

Fig. 7. DTA (curves 1a, 2a) and DTG (curves 1b, 2b) in air of green composite tapes prepared with different binders. 1a, 1b, poly(vinylbutyral) (PVB) based binder, 2a, 2b, polyacrylate (PAcr) based binder.

including opposite, superimposed DTA effects. Which of the effects prevails depends on the amount of oxygen available to react with the volatiles within the measuring system. At the decomposition rate maximum (DTG minimum) the oxidizable volatiles form so rapidly that there occurs a temporary shortage of oxygen in the sample crucible. The endothermic decomposition thus becomes dominant over exothermic oxidation, resulting in an endothermic peak.

This dramatic effect of gas exchange between sample and furnace atmosphere is modified by the arbitrary position of the sample fragments in the crucible, resulting in poor reproducibility of the shape of the DTA effects. This interpretation is in agreement with the finding that, at smaller heating rates (2.5 K min^{-1}, to increase the time for gas exchange) or with smaller samples (to reduce the amount of oxidizable volatiles), the endothermic peak disappeared.

To achieve a more continuous and complete binder burnout, the authors of [10] proposed reaction-controlled heating (RCH) instead of the usual linear heating programme. RCH resembles the techniques of "quasi-isothermal quasi-isobaric TG" [11] or "controlled rate thermal analysis" [12], in which the sample is heated (via certain feedback systems) in such a way that either (during decomposition steps) the mass loss rate $(dm/dt) = r = \text{const.}$, or (in those intervals where no mass loss occurs) the heating rate $(dT/dt) = \beta = \text{const.}$ Then, at a sufficiently low programmed mass loss rate r, residue-free oxidation of binder is anticipated. We did not follow this procedure.

Our TG results for the PVB binder are similar to those in [13], obtained with model ceramic oxide/PVB tapes of much lower (2%) binder content, which exhibited two-step degradation of PVB as well. With various ceramic oxide substrates, a different progress of combustion is reported [13], and is ascribed to the catalytic activity of the respective oxides. Our results suggest that gas exchange between the sample and the furnace atmosphere should also be taken into consideration.

In the following sections we compare a series of tapes prepared from the various AlN charges (Table 1), polyacrylate binder, and one glass (B 7/2.3), the raw mix ground to different particle sizes.

Curiously, the mass losses found with the polyacrylate tapes below 500°C are up to 1.5% greater than those calculated from their polymeric binder content. These differences between experiment and calculation, which increase with increasing specific surface of the raw mix, are not a part of the mass losses at < 150°C. Consequently they cannot be ascribed to the loss of residual solvents from the binder. Probably they are due to the elimination of moisture adsorbed either on AlN, where it may have reacted chemically to form aluminium hydroxide in the grinding process of the raw mix, or on the active glass surface generated by the milling process. It is likely that these additional mass losses are due to the grinding procedure rather than to the particle size of the starting materials. With the tape containing the surface-coated AlN charge WF this additional mass loss is also detected. We therefore prefer the explanation that the mass loss is due to desorption of moisture from the glass particles.

3.5. Further mass changes at > 500°C

After binder combustion, during the isothermal treatment at 500°C in air and upon further heating to ≈ 750°C, the pre-fired tapes exhibit very small mass losses $\leqslant 0.11$ mass%. Following the interpretation of [13], this should be due to the oxidation of carbonaceous residues formed by a side reaction accompanying the main oxidation of polymeric binder. Our TG results were obtained with binder concentrations nearly 10-fold higher than those in [13]. The amount of carbonaceous residue present at 500°C in our tapes was ≈ 0.5% of the original binder content, similar to that reported in [13].

When heated in air from 750 to 1150°C, tapes containing AlN show a slight mass increase of 0.05–0.10%. No mass increase is detected if heating is performed in an O_2-free atmosphere, or with tapes containing Al_2O_3 instead of AlN. These observations, together with the temperature interval, suggest that the mass gain is due to the oxidation of AlN (see "mass gain above 750°C", above). However, compared with pure AlN powder, the oxidation rate of AlN in the tape is smaller by a factor of < 0.1 (Fig. 8). Obviously the oxidation of AlN is drastically restricted by embedding the AlN particles in the glass matrix. Thus it is not necessary to fire the tapes at > 500°C at extremely low oxygen pressure to prevent excessive AlN oxidation. The corresponding expensive technological steps can be avoided. Both the mass loss at 505–750°C and the mass increase at > 750°C show no dependence on the AlN charge or the particle size of AlN or the raw mix.

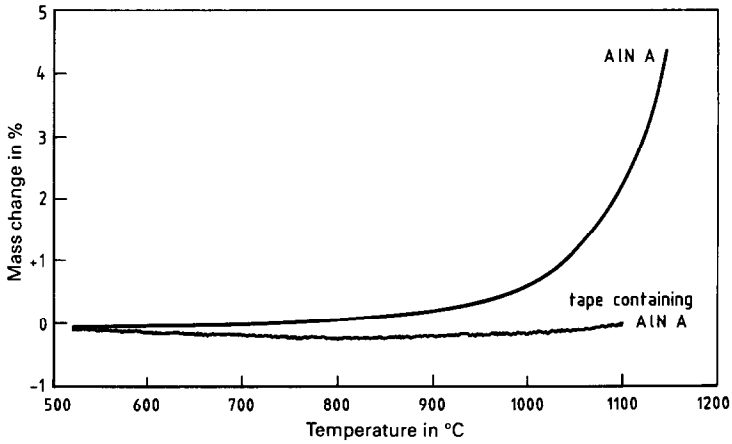

Fig. 8. TG curves (in air) of AlN powder (sample A) and a ceramic composite tape containing AlN A. Mass changes (%) of AlN content.

In contrast to the oxidation of free AlN powder, the antihydrolytic coating of charge WF does not retard the oxidation of AlN in the corresponding ceramic tape. Probably the coating is destroyed either by grinding the raw mix or by treatment with the organic binder.

3.6. Crystallization of the glass phase

The crystallization of cordierite from the glass phase is denoted by a relatively sharp exothermic effect at $\approx 920-1040$°C without any mass change. Compared with the crystallization of the pure glass powder (Fig. 9), the corresponding DTA exotherm of the tape is shifted to somewhat lower temperature, it becomes narrower and higher, and the peak area (relative to the amount of glass present in the composite, ≈ 55 mass% of the green tape) becomes larger. These differences suggest that the crystallization in the composite is accelerated and proceeds to a higher degree than in the glass powder. Extrapolated onset temperatures of crystallization in the series of tapes clearly decrease at decreasing particle size of the ceramic raw mix.

The influence of particle size of the glass outlined in section 3.2, and interpreted as being the result of heterogeneous nucleation on glass particle surfaces, contributes to the improvement of crystallization; however, it is accompanied by other, probably much stronger effects [14]. This is demonstrated in Fig. 10 and Table 8, which present the crystallization exotherms of glass powder, glass/Al_2O_3 (corundum), and glass/AlN composites, all with the same glass and equivalent particle size distribution. Obviously the crystallization temperature is decreased and the degree of crystallization is increased by the fillers Al_2O_3 and, more markedly, AlN. We ascribe this result to a phase boundary reaction between glass and filler, including the dissolution of Al_2O_3 or AlN in the glass. Because of the

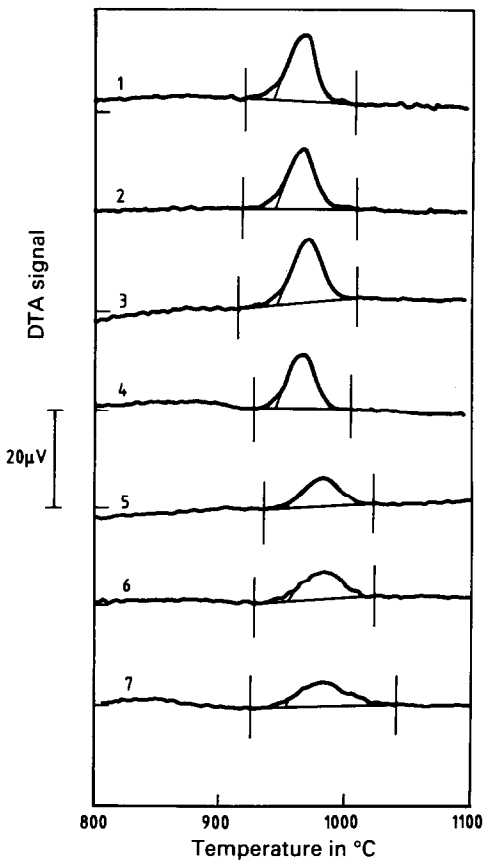

Fig. 9. DTA curves of cordierite crystallization of glass in tapes made from glass B 7/2.3 and different AlN charges and ground to different specific surfaces, and of pure glass powder of comparable specific surface (Table 7). 1, AlN F/S, $F_{BET} = 11.6$ m^2 cm^{-3}; 2, AlN B, $F_{BET} = 11.0$ m^2 cm^{-3}; 3, AlN WF, $F_{BET} = 10.8$ m^2 cm^{-3}; 4, AlN UF, $F_{BET} = 10.5$ m^2 cm^{-3}; 5, AlN A, $F_{BET} = 7.3$ m^2 cm^{-3}; 6, AlN UM, $F_{BET} = 6.8$ m^2 cm^{-3}; 7, glass B 7/2.3, 9.4 m^2 cm^{-3}.

resulting changes of the glass composition (a) the deficit of Al_2O_3 in the original glass limiting the crystallization ofcordierite is compensated, (b) nucleation and crystallization in the glass are stimulated by the incorporation of N^{3-} ions with a strong field, as known for other strong field ions, e.g. Ti^{4+}, Zr^{4+} or F^- [5].

4. Conclusions

TG–DTA measurements were performed on modern glass ceramic composite tapes consisting of AlN, a cordierite-forming silicate glass, a binder containing polymer and plasticizer, and a surfactant. Thermoanalytical results obtained with starting materials having different parameters (particle size, chemical composition)

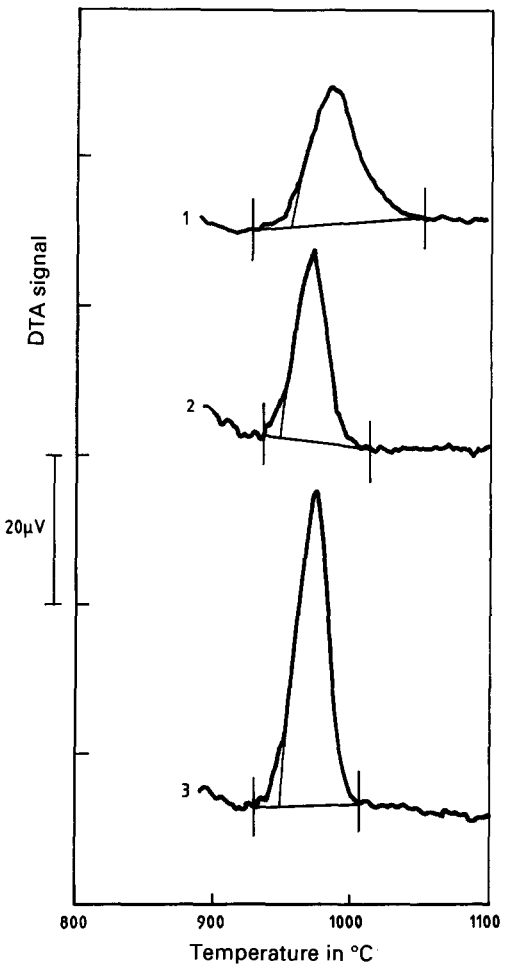

Fig. 10. DTA curves of cordierite crystallization of: 1, glass B 10 powder; 2, ceramic raw mixture B 10 + Al_2O_3; 3, ceramic raw mixture B 10 + AlN. Curves are normalized to glass content.

Table 8
DTA crystallization exotherms of glass B 10 and raw mixes of glass B 10 with Al_2O_3 or AlN

Sample	Glass B 10	B 10 + Al_2O_3	B 10 + AlN
extrapolated onset T_e/(°C)	953	946	948
peak maximum T_p/(°C)	982	970	973
Peak area:			
δH/(mV s g^{-1} sample)	122	70	111
δH/(mV s g^{-1} glass)	122	117	185

can be compared with each other and with those of the composite tape. They show the effect of surface coating of the AlN, the strong influence of the particle sizes of the glass and the AlN charge and the interaction of glass and AlN at high temperature.

Thermoanalytical measurements can be treated as a simulation of the ceramic firing process. Characteristic data concerning the progress and end temperature of binder combustion and glass crystallization behaviour are evaluated. The amount of carbonaceous residue and the degree and rate of AlN oxidation are estimated. The results can aid in optimizing the parameters of the technological firing process.

References

[1] J.I. Steinberg, S.J. Horowitz and R.J. Bacher, Solid State Technol., 1 (1986) 97.
[2] K. Kawakami, Adv. Ceram., 19 (1986) 95.
[3] M. Kirsch, H. Nieswand and W. Schiller, Silikattechnik, 41 (1991) 380.
[4] D.R. Hammond and S.W. Hankin, Thermochim. Acta, 192 (1991) 65.
[5] H. Rasch, in J. Kriegesmann (Ed.), Keramische Werkstoffe, 9. Erg.-Lfg., 1992, Chap. 4.1.3.0, p. 1. Deutscher Wirtschaftsdienst, Cologne.
[6] W. Zdaniewski, J. Am. Ceram. Soc., 58 (1975) 163.
[7] R. Müller, T. Hübert and M. Kirsch, Silikattechnik, 37 (1986) 111.
[8] K. Watanabe and E.A. Giess, J. Am. Ceram. Soc., 68 (1985) C102.
[9] K. Watanabe, E.A. Giess and M.W. Shafer, J. Mater. Sci., 20 (1985) 508.
[10] H. Verweij and W.H.M Bruggink, J. Am. Ceram. Soc., 73 (1990) 226.
[11] F. Paulik and J. Paulik, J. Therm. Anal., 5 (1973) 253.
[12] J. Rouquerol, Thermochim. Acta, 144 (1989) 209.
[13] S. Massia, P.D. Calvert, W.E. Rhine and H.K. Bowen, J. Mater. Sci., 24 (1989) 1907.
[14] W. Schiller, Ber.. Jahrestag. Dtsch. Keram. Ges., Weimar, Germany, October 1993, VDE, Berlin, 1993, p. 241.